Processing of graphene into a cantilever beam structure using a focused ion beam

Kazuma Matsui[1,*], *Yusuke Takei*[1,*], *Akira Inaba*[1], *Tomoyuki Takahata*[1], *Kiyoshi Matsumoto*[2], *Isao Shimoyama*[1] ✉

[1]*Department of Mechano-Informatics, The University of Tokyo, Tokyo, Japan 7-3-1 Hongo, Bunkyo-ku, Tokyo 113-8656, Japan*
[2]*Department of Mechanical Engineering, Faculty of Science and Engineering, Toyo University, 2100 Kujirai, Kawagoe-shi, Saitama 350-8585, Japan*
[*]*These authors contributed equally to this work.*
✉ *E-mail: issh@leopard.t.u-tokyo.ac.jp*

Published in Micro & Nano Letters; Received on 26th April 2016; Revised on 27th June 2016; Accepted on 29th June 2016

A graphene cantilever beam of arbitrary shape by patterning suspended graphene using a focused ion beam (FIB) is fabricated. Suspended graphene was formed by transferring graphene over a trench structure and patterned the suspended graphene into a cantilever beam structure. When the suspended graphene is patterned by an FIB, the high-ion irradiation of FIB deforms the shape of the cantilever beam; in contrast, low-ion irradiation cannot penetrate the suspended graphene. An evaluation of the ion irradiation dose of the FIB and the damages caused to the suspended graphene confirmed that in the case of few-layer graphene with a maximum of three layers, optimum processing can be performed by an ion irradiation of 6×10^{16} ions/cm^2. Under this condition, a graphene cantilever beam with a width of 1.34 μm and a length of 2.13 μm could be fabricated. Furthermore, the Raman spectroscopy results indicate that the FIB process does not significantly change the properties of the graphene.

1. Introduction: Nanosized cantilever beams are expected to be applied in a variety of fields. For example, a cantilever beam is expected to be used as a nanosize mechanical resonator to measure radiation pressure noise [1, 2]. Furthermore, nanosized cantilever beams, which generate large displacement motions with respect to force, are expected to be applicable to atomic force microscopes, magnetic force microscopes, magnetic resonance force microscopes, and similar measuring instruments [3–6]. In addition, graphene is considered to be desirable optoelectronic–mechanic devices, because of its tunable spatially varying bandgap property [7, 8]. In recent years, graphene has become a candidate material for nanosized cantilever structures [1, 4, 9–11]. It is expected that a cantilever beam of thickness <1 nm can be realised based on graphene; however, current technologies cannot achieve a graphene cantilever beam having an arbitrary shape at a desired location with a sufficiently high yield.

One conventional method for fabricating a graphene cantilever beam involves transferring graphene onto a substrate that has a hole [1, 9, 12–14]. This approach is based on the fact that graphene pieces are formed by accidental breaking during the transfer, leading to a variety of pieces being transferred over the hole. However, because the graphene breaking positions cannot be selected in this manner, the yield is low and it is impossible to fabricate a graphene cantilever beam with an arbitrary width and length. To use a graphene cantilever beam for applications such as resonators, it is necessary to process graphene into any desired shape to obtain the physical characteristics corresponding to the technical specifications.

This Letter aimed to fabricate a graphene cantilever beam of arbitrary shape by patterning suspended graphene using a focused ion beam (FIB). Graphene is transferred over a trench structure created on a silicon (Si) substrate to form suspended graphene, and then FIB irradiation is used to etch a portion of the graphene membrane to fabricate a graphene cantilever beam structure having an arbitrary width and length (Fig. 1). In previous studies, FIBs have also been used to process suspended graphene; however, designed shapes could not be realised because the FIB process was not optimised with respect to the ion irradiation dose [15, 16]. Therefore, the patterning was limited to simple shapes such as a circle or straight line [17]. In our previous work, we fabricated a graphene cantilever beam via FIB irradiation of suspended graphene and measured the resonant frequency of the cantilever beam [10]. However, we did not optimise the FIB irradiation dose; as a result, the fabricated cantilever beam had a curved edge shape. In this Letter, we examined the relationship between the FIB irradiation dose and the cut shape of membrane-structured graphene. In addition, we sought to pattern graphene cantilever beam shapes by adopting the optimum FIB irradiation conditions for processing few-layer graphene (FLG).

2. Fabrication method: The process used to fabricate graphene cantilever beam structures in this Letter is illustrated in Fig. 2. In the graphene growing process shown in Figs. 2*a*1 and *a*2, FLG is grown on a copper foil via chemical vapour deposition (CVD). Fig. 3 shows the CVD setup for growing graphene. Ethanol was used as the carbon source, and copper foil was used as the catalyst. Using this setup, ethanol vapour and argon gas containing 3% hydrogen can be supplied. The copper foil was introduced into a quartz tube and annealed for 10 min by heating to 900°C with a heater in an argon–hydrogen atmosphere. Thereafter, while stopping the gas and maintaining a temperature of 900°C, ethanol gas was allowed to flow for 5 min. After

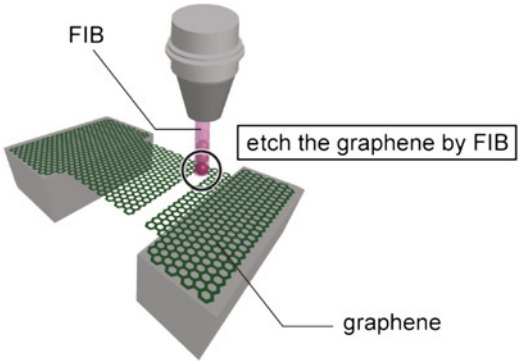

Fig. 1 *Conceptual image of graphene cantilever beam processing using an FIB*

doi: 10.1049/mnl.2016.0198

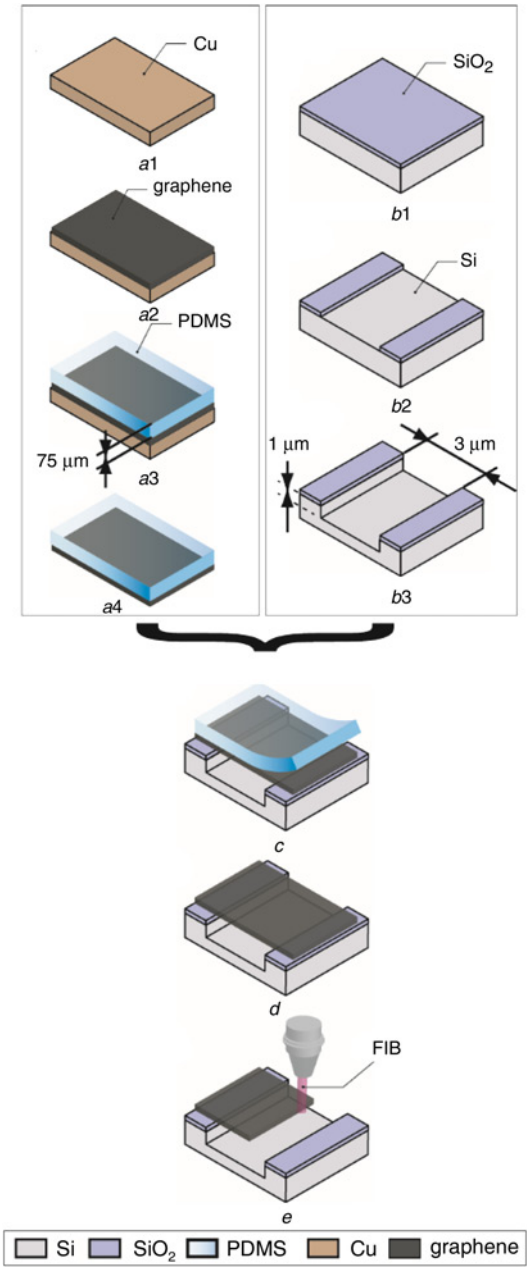

Fig. 2 *Fabrication process of a graphene cantilever beam*
*a*1 Preparing cupper foil
*a*2 Growing graphene on surface of the cupper foil via CVD
*a*3 Contacting a PDMS on the graphene
*a*4 Etching the cupper foil
*b*1 Preparing SiO_2/Si wafer
*b*2 Patterned the SiO_2 layer
*b*3 Fabricating trench structure by etching the Si layer
c Contacting the PDMS with transferred graphene to the Si trench structure
d Peeling off the PDMS from the transferred graphene
e Patterning graphene into cantilever shape by FIB

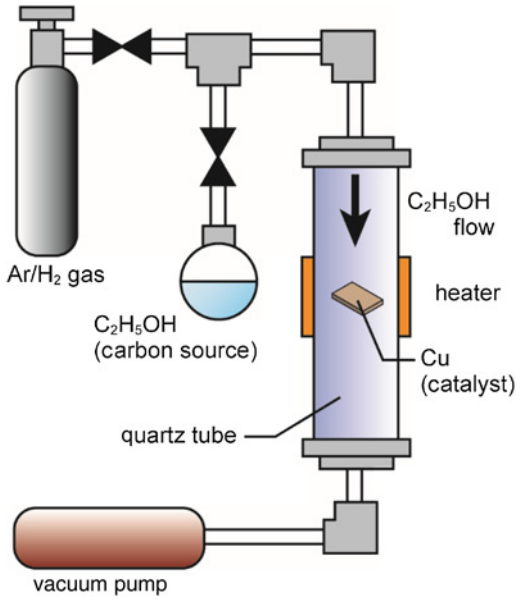

Fig. 3 *Alcohol CVD setup for synthesising graphene*

stopping the flow of the ethanol gas, the heater was switched off and the system was cooled while argon–hydrogen gas was allowed to flow for 7 min at a flow rate of 300 sccm. In this cooling process, the carbon that diffused into the catalyst was crystallised on the surface of the copper foil to form FLG with 1–3 layers [18–20]. Subsequently, in the step shown in Figs. 2*a*3 and *a*4, the graphene on the copper foil was transferred to polydimethylsiloxane (PDMS). First, a film was formed on a 3 × 4 cm glass substrate by spin-coating PDMS at 1000 rpm for 10 s. After contacting the copper foil covered by graphene with PDMS, the glass substrate was placed on a hot plate at 70°C for 30 min to cure the PDMS. Finally, the copper was etched by immersing the glass substrate in a copper etchant (ferric chloride solution with a concentration of 38%) at 45°C for 50 min, thereby leaving only graphene on the PDMS layer [21].

In the process shown in Figs. 2*b*1–*b*3, after forming a trench with a width of 3 μm and a depth of 1 μm by etching an SiO_2/Si wafer, the graphene on PDMS was transferred over the trench structure via the steps shown in Figs. 2*c* and *d*. Pure water droplets were dropped onto the SiO_2/Si wafer with the trench structure, and the PDMS with the transferred graphene was placed on top of the droplets with the graphene surface down. After evaporating the liquid drops on a hot plate at 70°C, the piece was allowed to stand for 24 h. Next, by immersing the Si wafer with the PDMS into acetone maintained at 70°C, the PDMS was peeled off from the wafer to obtain a piece of suspended graphene. Atomic force microscopy (AFM) measurements indicated that the thickness of the graphene transferred onto the SiO_2 was 1 nm. According to the previous research, the height of monolayer graphene on SiO_2 measured by AFM has been often reported higher than the graphite inter-layer separation [22, 23]. Thus the transferred graphene was estimated to have bilayer.

Finally, in the step shown in Fig. 2*e*, the graphene was cut by an FIB (XVision200TB, Hitachi High-Tech Science, Japan) to process the graphene into a cantilever beam structure. The FIB processing conditions used in this Letter are provided in Table 1: an acceleration voltage of 30 keV, a beam current of 11.7 pA, a beam diameter of 14 nm, and a beam dwell time of 50 μs. The ion irradiation dose of the FIB was adjusted (as described in the next section) to cut to a level of 6×10^{16} ions/cm^2.

3. Experiments

3.1. Evaluation of FIB irradiation and the processed graphene: When processing suspended graphene by an FIB, an area larger than the beam diameter may be removed if the ion irradiation dose of the FIB is excessively high. To clarify this phenomenon, some researchers verified lateral damage in graphene carved by FIB [24, 25], and concluded that scattering of the Ga ions in the residual gas causes the carving around the FIB-irradiated area. Furthermore, when processing the suspended graphene with FIB, the residual stress of the graphene film when transferring onto the substrate causes the cut surface resulting in up-curled shape [12, 26]. In contrast, when processing the graphene transferred on the

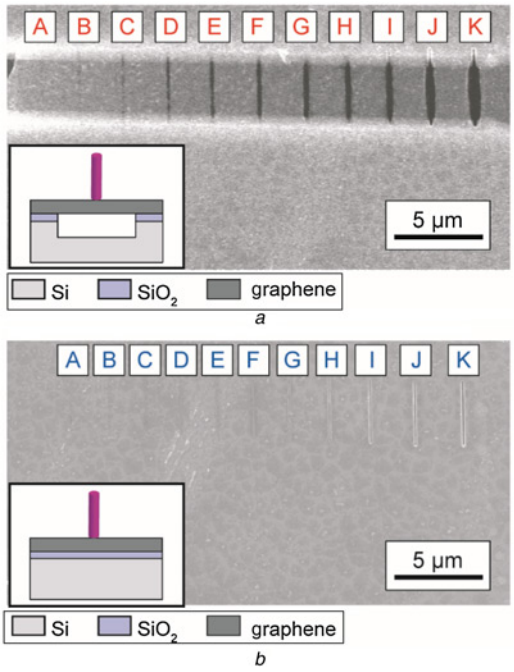

	ion irradiation dose, ions/cm²		ion irradiation dose, ions/cm²
A	1.9×10^{15}	F	6.0×10^{16}
B	3.8×10^{15}	G	1.2×10^{17}
C	7.6×10^{15}	H	2.4×10^{17}
D	1.5×10^{16}	I	4.8×10^{17}
E	3.0×10^{16}	J	9.6×10^{17}
		K	1.9×10^{18}

c

Fig. 4 *Lines drawn on suspended graphene and graphene on SiO_2 with changing the FIB ion irradiation dose*
a FIB exposure on suspended graphene
b FIB exposure on graphene fixed on SiO_2
c Ion irradiation dose at (*a*), (*b*)

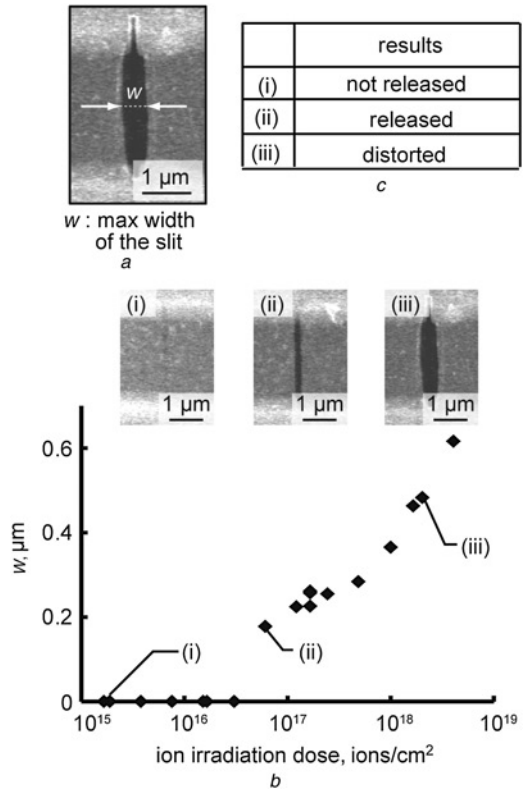

Fig. 5 *Evaluation of the relationship between the amount of deformation and the FIB ion irradiation dose*
a Enlarged view of the slit (*w* is defined as the max width of the slit)
b Relationship between *w* and ion irradiation dose
c The condition of the resulting slit

substrate, contacting force between graphene and the substrate is thought to be larger than the residual stress of the graphene, the cut surface of the graphene is in contact with the substrate. Additionally, the cut surface may become curved even when scanning beams are moved along a straight line. On the other hand, when the ion irradiation dose of the FIB is overly small, the beam cannot remove the graphene. In particular, because this Letter intended to use FIB processing on FLG with a maximum of three layers, which is thinner than the graphene used in previous works, an appropriate dose had to be estimated based on the ion irradiation dose when processing the graphene by the FIB and the removed graphene shape. Therefore, experiments were conducted to verify the relationship between the ion irradiation dose and removed graphene shape.

Figs. 4*a* and *b* show the scanning electron microscopy (SEM) images obtained when suspended graphene and graphene fixed on SiO_2 were irradiated with ion irradiation doses in the range of 2×10^{15}–2×10^{18} ions/cm^2 to form a linear pattern of 0.1 μm in width and 2.7 μm in length. The FIB processing conditions are shown in Table 1. In Figs. 4*a* and *b*, the FIB-irradiated line patterns were assigned symbols from A to K, and in each image the same symbols correspond to the same ion irradiation dose. The ion irradiation doses from A to K are shown in Fig. 4*c*. As shown in Figs. 4*a* and *b*, the suspended graphene underwent large deformation due to FIB irradiation compared with the graphene fixed on the SiO_2 surface. The extent of deformation increased with the dose, particularly for the high-ion irradiation dose.

Table 1 FIB conditions for processing graphene

acceleration voltage	30 keV
beam current	11.7 pA
beam size	14 nm
dwell time	50 μs

The maximum width *w* of the slit on the suspended graphene made by FIB ion irradiation was measured to evaluate the amount of deformation that occurred during FIB irradiation, as shown in Fig. 5*a*. To pattern suspended graphene into cantilever of arbitrary shape, *w* must be minimised. The relationship between *w* and the ion irradiation dose is shown in Figs. 5*b* and *c*. As shown in Fig. 5*b*, cutting cannot be achieved completely when the ion irradiation dose is 6×10^{16} ions/cm^2 or less, whereas graphene is completely cut with an ion irradiation dose exceeding 6×10^{16} ions/cm^2, and *w* increases as the ion dose increases. The above results illustrate that cutting of the smallest *w* of 0.18 μm could be achieved when processing with an ion irradiation dose of 6×10^{16} ions/cm^2. Furthermore, under such irradiation conditions, an ion beam with a width of 0.1 μm was irradiated to form a linear slit with a maximum width of 0.18 μm, i.e. a linear shape 0.08 μm larger than the designed size was produced. In other words, when performing FIB irradiation, which processes both separated sides of the suspended graphene, the size is reduced by ~0.04 μm per side.

3.2. Processing a cantilever beam structure by an FIB: Fig. 6 shows the FIB processing procedure used to fabricate a cantilever beam of graphene from suspended graphene. First, ions were irradiated in a line shape that was 0.1 μm wide and 2.7 μm long to cut the suspended graphene into a double supported beam structure (Fig. 6*a*). Subsequently, the suspended graphene near the double

doi: 10.1049/mnl.2016.0198

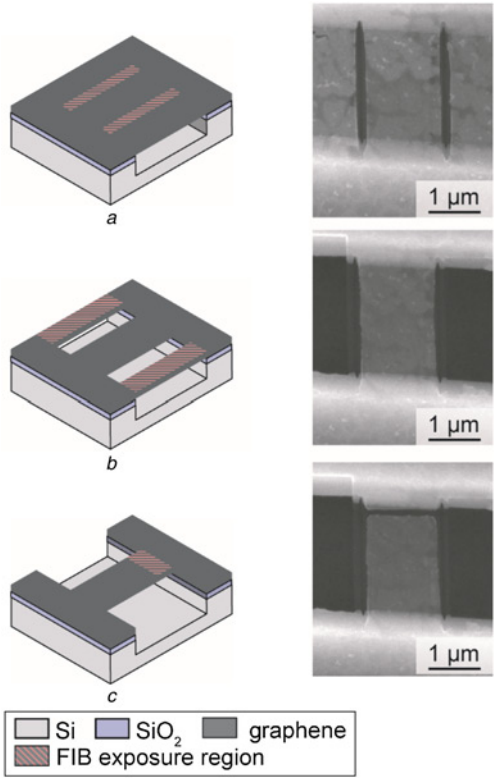

Fig. 6 *Schematics and SEM images of a graphene cantilever beam formed by the FIB irradiation of suspended graphene*
a Patterning graphene beam
b Removing suspended graphene near the beam
c Patterning graphene cantilever

supported beam was removed by the FIB (Fig. 6*b*). Thereafter, the tip of the graphene double supported beam was cut along a line with a width of 0.1 μm and length of 2.0 μm to produce a cantilever beam structure (Fig. 6*c*).

The fabricated graphene cantilever beam is shown in Fig. 7. The designed cantilever beam was 1.43 μm wide and 2.16 μm long. The finished cantilever beam fabricated by FIB irradiation with an ion irradiation dose of 6×10^{16} ions/cm^2 was ∼1.34 μm wide and ∼2.13 μm long. The difference from the design values was ∼0.09 μm shorter in the width direction and ∼0.03 μm shorter in the length direction. That is, for each side of graphene, the processed value was ∼0.045 μm shorter in the width direction and ∼0.03 μm shorter in the length direction. This result is highly consistent with the results of ⟨3.1⟩, demonstrating that fabrication was achieved with a 0.04 μm in thickness per side.

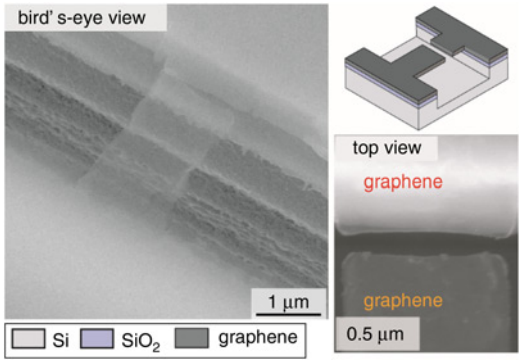

Fig. 7 *SEM images of a fabricated graphene cantilever beam*

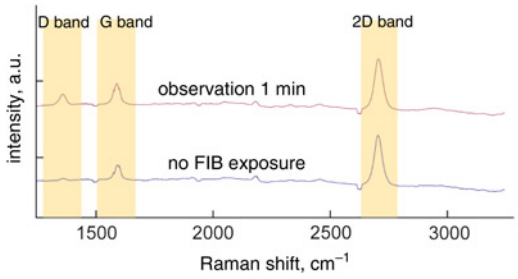

Fig. 8 *Raman spectra of monolayer graphene on SiO_2 before and after FIB irradiation*

Furthermore, when processing graphene via FIB irradiation, we determined a processing position by observing a sample surface by FIB irradiation for ∼10 s while generating secondary electrons. Though the irradiation dose for the observation is small compared with that in the duration of processing, there is a risk of damaging the graphene. Therefore, the graphene surface was evaluated by Raman spectroscopy (Fig. 8). We used 40 mW Ar ion laser, which has wavelength of 488 nm, as a light source. Moreover, spectroscopic measurement was conducted with spectrograph (Acton Spectrapro 2300i, Princeton Instruments, USA). The Raman spectra of monolayer graphene on SiO_2 after FIB irradiation are shown in Fig. 8. Here, (a) shows the spectrum in the absence of FIB irradiation and (b) is the spectrum obtained after 1 min of observation, longer than the normal observation time of 10 s. Considering that there is no large change in the Raman spectrum after 1 min of FIB observation, the graphene does not experience severe damage due to an observation of ∼10 s during FIB processing. Thus, in the proposed graphene fabrication process using an FIB, processing can be achieved while maintaining the properties of the graphene.

4. Conclusion: In this Letter, a graphene cantilever beam structure was produced with the designed width and length. Evaluation of the ion irradiation dose of FIB and the damage caused to the suspended graphene indicated that in the case of FLG with a maximum of three layers, optimum patterning can be performed using an ion irradiation dose of 6×10^{16} ions/cm^2. Using this FIB dose, a graphene cantilever beam with a width of 1.34 μm and a length of 2.13 μm was fabricated. Furthermore, according to the Raman spectroscopy results, no substantial change in the properties of graphene occurs by observing the graphene for ∼10 s using an FIB.

5. Acknowledgment: This study was partially supported by Japan Society for the Promotion of Science (JSPS) KAKENHI under grant no. 25000010.

6 References

[1] Rasuli R., Iraji Zad A., Ahadian M.M.: 'Mechanical properties of graphene cantilever from atomic force microscopy and density functional theory', *Nanotechnology*, 2010, **21**, (18), pp. 185503
[2] Castellanos-Gomez A., Singh V., van der Zant H.S.J., *ET AL.*: 'Mechanics of freely-suspended ultrathin layered materials', *Ann. Phys. (Berlin)*, 2015, **527**, (1–2), pp. 27–44
[3] Igaki J., Nakamatsu K., Kometani R., *ET AL.*: 'Mechanical characteristics and applications of diamond like-carbon cantilevers fabricated by focused-ion-beam chemical vapor deposition', *J. Vac. Sci. Technol. B*, 2006, **24**, (6), pp. 2911–2914
[4] Bunch J.S., van der Zande A.M., Verbridge S.S., *ET AL.*: 'Electromechanical resonators from graphene sheets', *Science*, 2007, **315**, (5811), pp. 490–493
[5] Anetsberger G., Arcizet O., Unterreithmeier Q.P., *ET AL.*: 'Near-field cavity optomechanics with nanomechanical oscillators', *Nat. Phys.*, 2009, **5**, (12), pp. 909–914

[6] Ilic B., Krylov S., Craighead H.G.: 'Theoretical and experimental investigation of optically driven nanoelectromechanical oscillators', *J. Appl. Phys.*, 2010, **107**, (3), pp. 034311
[7] Feng J., Qian X.F., Huang C.W., *ET AL.*: 'Strain-engineered artificial atom as a broad-spectrum solar energy funnel', *Nat. Photonics*, 2012, **6**, (12), pp. 865–871
[8] van der Zande A., Hone J.: 'Optical Materials Inspired by strain', *Nat. Photonics*, 2012, **6**, (12), pp. 803–805
[9] Reserbat-Plantey A., Marty L., Arcizet O., *ET AL.*: 'A local optical probe for measuring motion and stress in a nanoelectromechanical system', *Nat. Nanotechnol.*, 2012, **7**, (3), pp. 151–155
[10] Matsui K., Inaba A., Oshidari Y., *ET AL.*: 'Mechanical properties of few layer graphene cantilever'. 2014 IEEE 27th Int. Conf. on Micro Electro Mechanical Systems (MEMS), San Francisco, CA, 2014, pp. 1087–1090
[11] Li P., You Z., Cui T.H.: 'Graphene cantilever beams for nano switches', *Appl. Phys. Lett.*, 2012, **101**, p. 093111
[12] Meyer J.C., Geim A.K., Katsnelson M.I., *ET AL.*: 'The structure of suspended graphene sheets', *Nature*, 2007, **446**, (7131), pp. 60–63
[13] Hemamouche A., Morin A., Bourhis E., *ET AL.*: 'FIB patterning of dielectric, metallized and graphene membranes: a comparative study', *Microelectron. Eng.*, 2014, **121**, pp. 87–91
[14] Lee C., Wei X., Kysar J.W., *ET AL.*: 'Measurement of the elastic properties and intrinsic strength of monolayer graphene', *Science*, 2008, **321**, (5887), pp. 385–388
[15] Lucot D., Gierak J., Ouerghi A., *ET AL.*: 'Deposition and FIB direct patterning of nanowires and nanorings into suspended sheets of graphene', *Microelectron. Eng.*, 2009, **86**, (4–6), pp. 882–884
[16] Oshidari Y., Hatakeyama T., Kometani R., *ET AL.*: 'High quality factor graphene resonator fabrication using resist shrinkage-induced strain', *Appl. Phys. Express*, 2012, **5**, (11), pp. 117201
[17] Morin A., Lucot D., Ouerghi A., *ET AL.*: 'FIB carving of nanopores into suspended graphene films', *Microelectron. Eng.*, 2012, **97**, pp. 311–316
[18] Maruyama S., Kojima R., Miyauchi Y., *ET AL.*: 'Low-temperature synthesis of high-purity single-walled carbon nanotubes from alcohol', *Chem. Phys. Lett.*, 2002, **360**, (3–4), pp. 229–234
[19] Li X., Cai W., An J., *ET AL.*: 'Large-area synthesis of high-quality and uniform graphene films on copper foils', *Science*, 2009, **324**, (5932), pp. 1312–1314
[20] Liao C.D., Lu Y.Y., Tamalampudi S.R., *ET AL.*: 'Chemical vapor deposition synthesis and Raman spectroscopic characterization of large-area graphene sheets', *J. Phys. Chem. A*, 2013, **117**, (39), pp. 9454–9461
[21] Yoo K., Takei Y., Kim S., *ET AL.*: 'Direct physical exfoliation of few-layer graphene from graphite grown on a nickel foil using polydimethylsiloxane with tunable elasticity and adhesion', *Nanotechnology*, 2013, **24**, (20), p. 205302
[22] Nemes-Incze P., Osvath Z., Kamaras K., *ET AL.*: 'Anomalies in thickness measurements of graphene and few layer graphite crystals by tapping mode atomic force microscopy', *Carbon*, 2008, **46**, (11), pp. 1435–1442
[23] Ni Z.H., Wang H.M., Kasim J., *ET AL.*: 'Graphene thickness determination using reflection and contrast spectroscopy', *Nano Lett.*, 2007, **7**, (9), pp. 2758–2763
[24] Liao Z.Q., Zhang T., Gall M., *ET AL.*: 'Lateral damage in graphene carved by high energy focused gallium ion beams', *Appl. Phys. Lett.*, 2015, **107**, 013108
[25] Thissen N.F.W., Vervuurt R.H.J., Mulders J.J.L., *ET AL.*: 'The effect of residual gas scattering on Ga ion beam patterning of graphene', *Appl. Phys. Lett.*, 2015, **107**, p. 213101
[26] Shivaraman S., Barton R.A., Yu X., *ET AL.*: 'Free-standing epitaxial graphene', *Nano Lett.*, 2009, **9**, (9), pp. 3100–3105

doi: 10.1049/mnl.2016.0198